Technical Report SL-97-12
October 1997

US Army Corps of Engineers
Waterways Experiment Station

Hydraulic Forces on a Wicket Gate Under Upstream Quasi-Laminar Flow

An Experimental Analysis Technique

by Luis A. de Béjar

Prepared for Headquarters, U.S. Army Corps of Engineers

The contents of this report are not to be used for advertising, publication, or promotional purposes. Citation of trade names does not constitute an official endorsement or approval of the use of such commercial products.

The findings of this report are not to be construed as an official Department of the Army position, unless so designated by other authorized documents.

Technical Report SL-97-12
October 1997

Hydraulic Forces on a Wicket Gate Under Upstream Quasi-Laminar Flow

An Experimental Analysis Technique

by Luis A. de Béjar

U.S. Army Corps of Engineers
Waterways Experiment Station
3909 Halls Ferry Road
Vicksburg, MS 39180-6199

Final report

Approved for public release; distribution is unlimited

Prepared for U.S. Army Corps of Engineers
Washington, DC 20314-1000

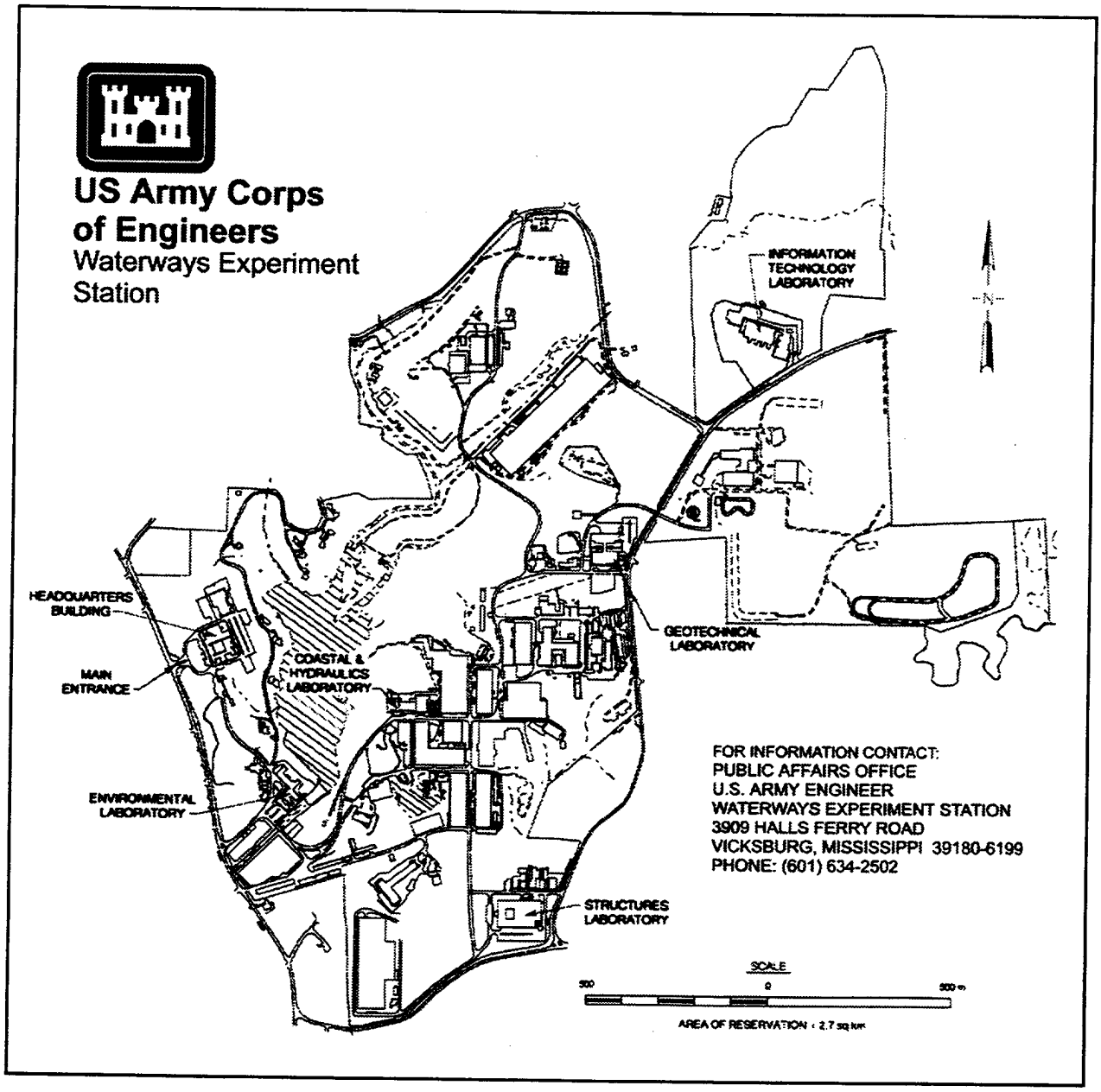

Waterways Experiment Station Cataloging-in-Publication Data

Bejar, Luis A. de.

Hydraulic forces on a wicket gate under upstream quasi-laminar flow : an experimental analysis technique / by Luis A. de Bejar ; prepared for U.S. Army Corps of Engineers.

41 p. : ill. ; 28 cm. — (Technical report ; SL-97-12)

Includes bibliographical references.

1. Hydraulic gates. 2. Streamflow. 3. Laminar flow. I. United States. Army. Corps of Engineers. II. U.S. Army Engineer Waterways Experiment Station. III. Structures Laboratory (U.S. Army Engineer Waterways Experiment Station) IV. Title. V. Series: Technical report (U.S. Army Engineer Waterways Experiment Station) ; SL-97-12.

TA7 W34 no.SL-97-12

Contents

List of Figures

Preface

This study on the experimental analysis of hydraulic forces on a wicket gate under upstream quasi-laminar flow was sponsored by the Department of the Army and is part of ongoing program of research in Civil Works on Hydraulic Structures. The investigation was conducted by members of the staff of the Structures Laboratory (SL) through the Research Program on Structural Engineering, Flow-Induced Vibrations of Gates, at the U.S. Army Engineer Waterways Experiment Station (WES) during the period October 1994 to August 1996 under the direction of Mr. Bryant Mather, Director, SL; Mr. John Ehrgott, Assistant Director, SL; and under the general supervision of Dr. Reed Mosher, Chief, Structural Mechanics Division, SL, and Dr. R. L. Hall, Structural Analysis Group, SL.

This report was written by Dr. Luis A. de Béjar, SL. The physical experiments were a coordinated effort between Mr. G. W. Davis, Hydraulics Laboratory, Dr. M. R. Chowdhury, SL, and Mr. H. C. Greer III, Instrumentation Services Division, Information Technology Laboratory. Mr. Lucian Guthrie and Mr. Don Dressler, Headquarters, U.S. Army Corps of Engineers, were Technical Monitors of the Research Program on Structural Engineering.

At the time of publication of this report, Director of WES was Dr. Robert W. Whalin. Commander was COL Robin R. Cababa, EN.

1 Introduction

Hydraulic wicket gates are modern appurtenances for flow control at locks-and-dam systems while maintaining the navigational characteristics of a pass. Structurally, these gates are a group of edge-hinged steel panels acting in parallel and independently driven by remote-controlled hydraulic actuators. The gates operate from a horizontal open position to an engineered elevation in the closed-gate condition. Due to complex surrounding flow, individual gates are subjected to hydraulic forces which locally compound the steady-state component of the induced stresses with random fluctuations.

The Olmsted locks-and-dam system will use 220 hydraulic wickets for navigational flow control of the Ohio River at Paducah, KY (March and Elder 1992). This report describes the experimental analysis to define a mathematical model to estimate the hydraulic forces on a prototypical Olmsted wicket gate under upstream quasi-laminar flow. In the mathematical model, water is assumed an ideal homogeneous, incompressible and inviscid fluid, and its flow is taken as irrotational. Quasi-laminar flow is defined as flow associated with small to moderate velocities (Reynolds' number smaller than approximately 2000 (Tritton 1982)).

The hydraulic environment in which water flows through a three-gate aperture and subsequently impinges on a single central gate in closed position (60° eleva-tion) was identified from experimentation on a corresponding 1/25-scale physical model at the U.S. Army Engineer Waterways Experiment Station (WES) as one of the critical conditions to be considered in the gate design.

Figures 1 through 3 illustrate the setup for the experiments. Figure 1 shows the dry physical model, Figure 2 illustrates an instance of quasi-laminar flow through a three-gate aperture, and Figure 3 illustrates the quasi-laminar hydraulic environment acting on a wicket gate at 45° elevation.

2 Theoretical Development

Eccentricity of the Conics

The notion of eccentricity (or flatness) of the conics is briefly reviewed and summarized as the starting step of the development (Kreyszig 1988).

Ellipse

Figure 4a shows a general ellipse with equation:

$$\frac{x^2}{s^2} + \frac{y^2}{t^2} = 1 \tag{1}$$

where s and t are the major and minor semiaxes, respectively.

Points P on the ellipse have the property that the sum of the distances from P to the foci (F_1 and F_2) is constant. The value of this constant is apparent when the end A of the major semiaxis is considered:

$$d_1 + d_2 = 2s \tag{2}$$

Consideration of end B of the minor semiaxis leads to an expression for the focal distance c:

$$c = \sqrt{s^2 - t^2} \tag{3}$$

where $s > c$.

The eccentricity of the ellipse is defined as:

$$e = \frac{c}{s} = \cos\theta \leq 1 \tag{4}$$

The completely nonflat ellipse is a circle, for which $e = 0$, and the completely flat ellipse is the focal segment F_1F_2, for which $e = 1$.

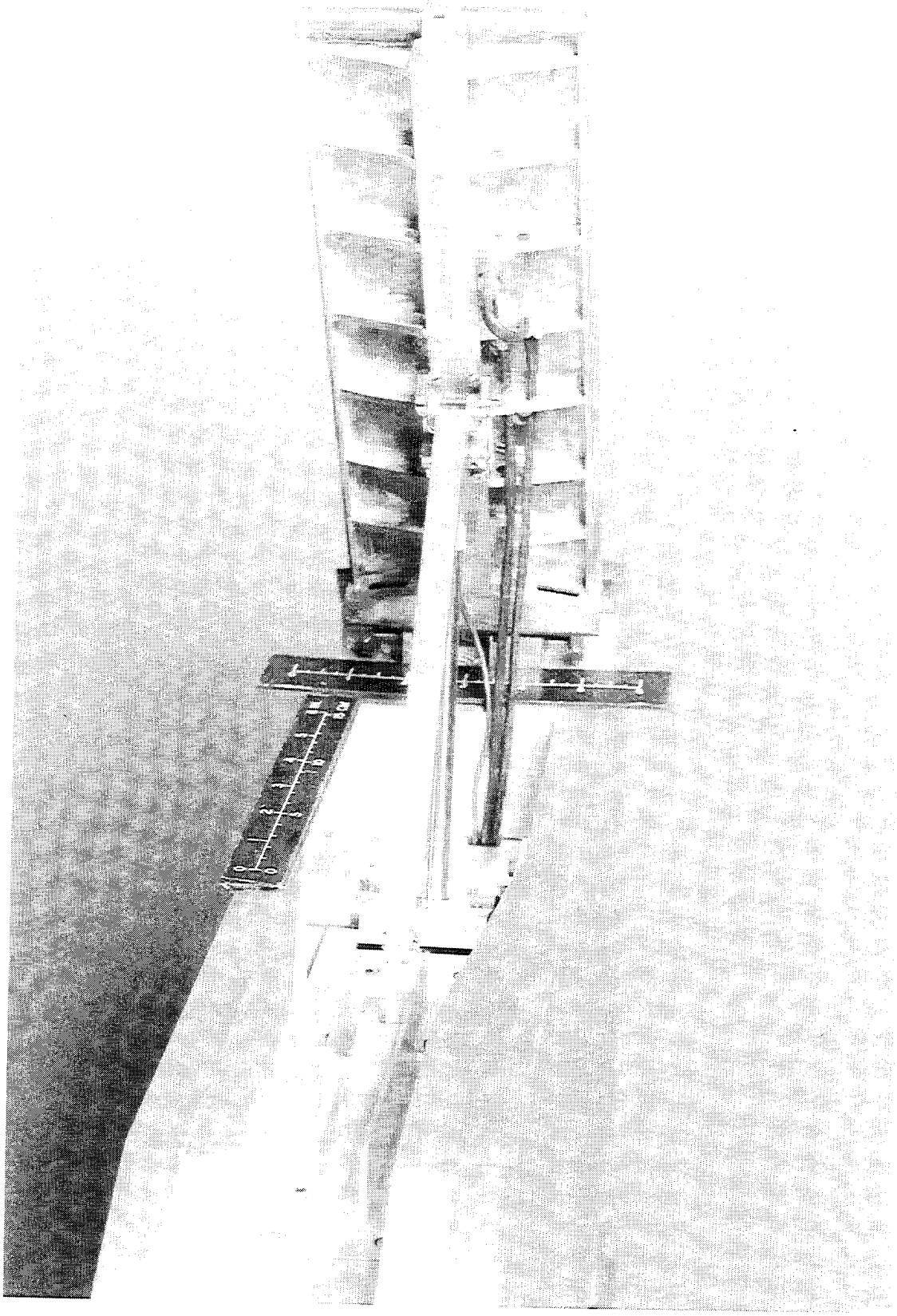

Figure 1. Physical model of Olmsted wicket gate (Scale 1:25)

Figure 2. Free physical flow through three-gate aperture at boundary of reservoir

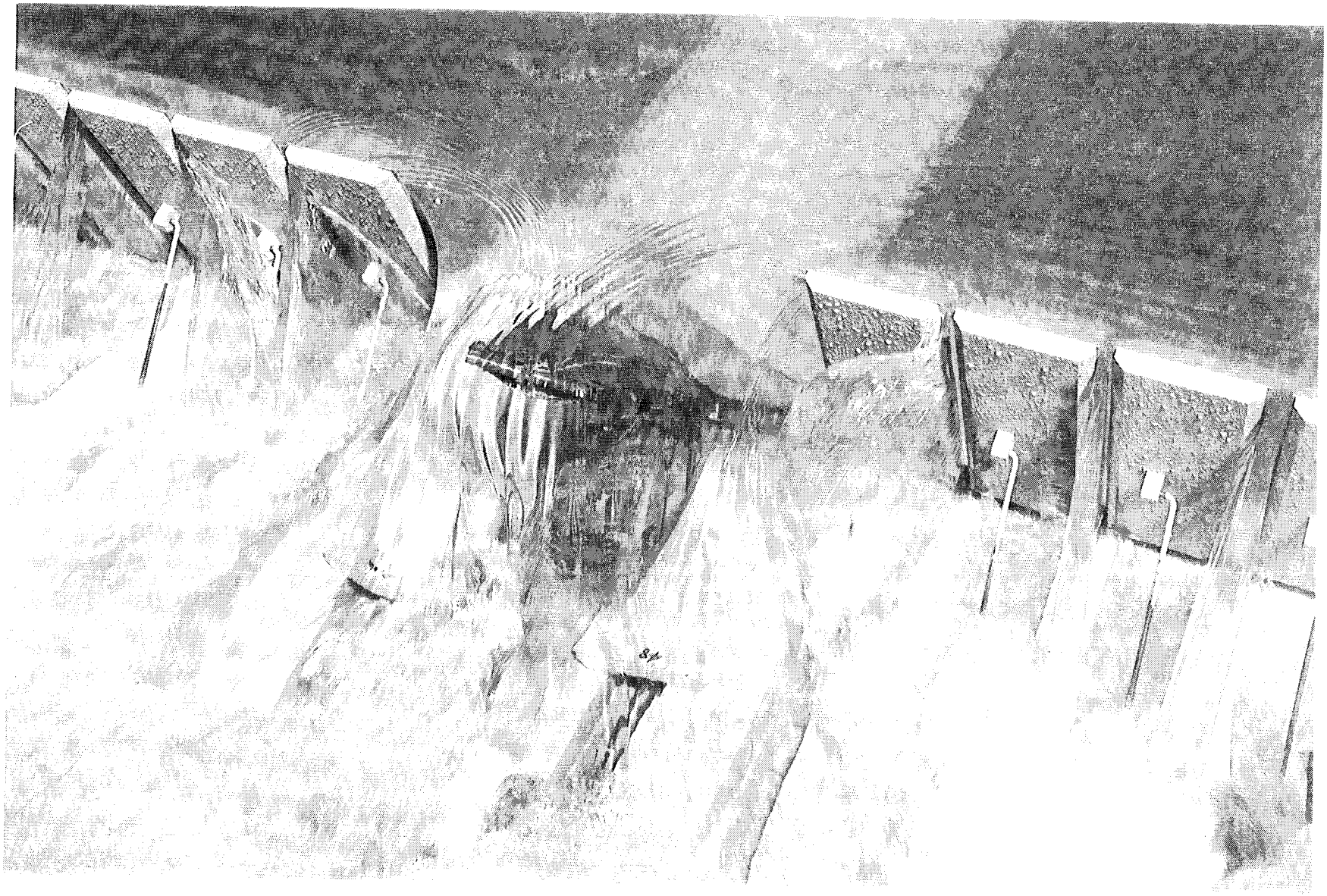

Figure 3. Physical flow through three-gate aperture impinging wicket gate at 45° elevation

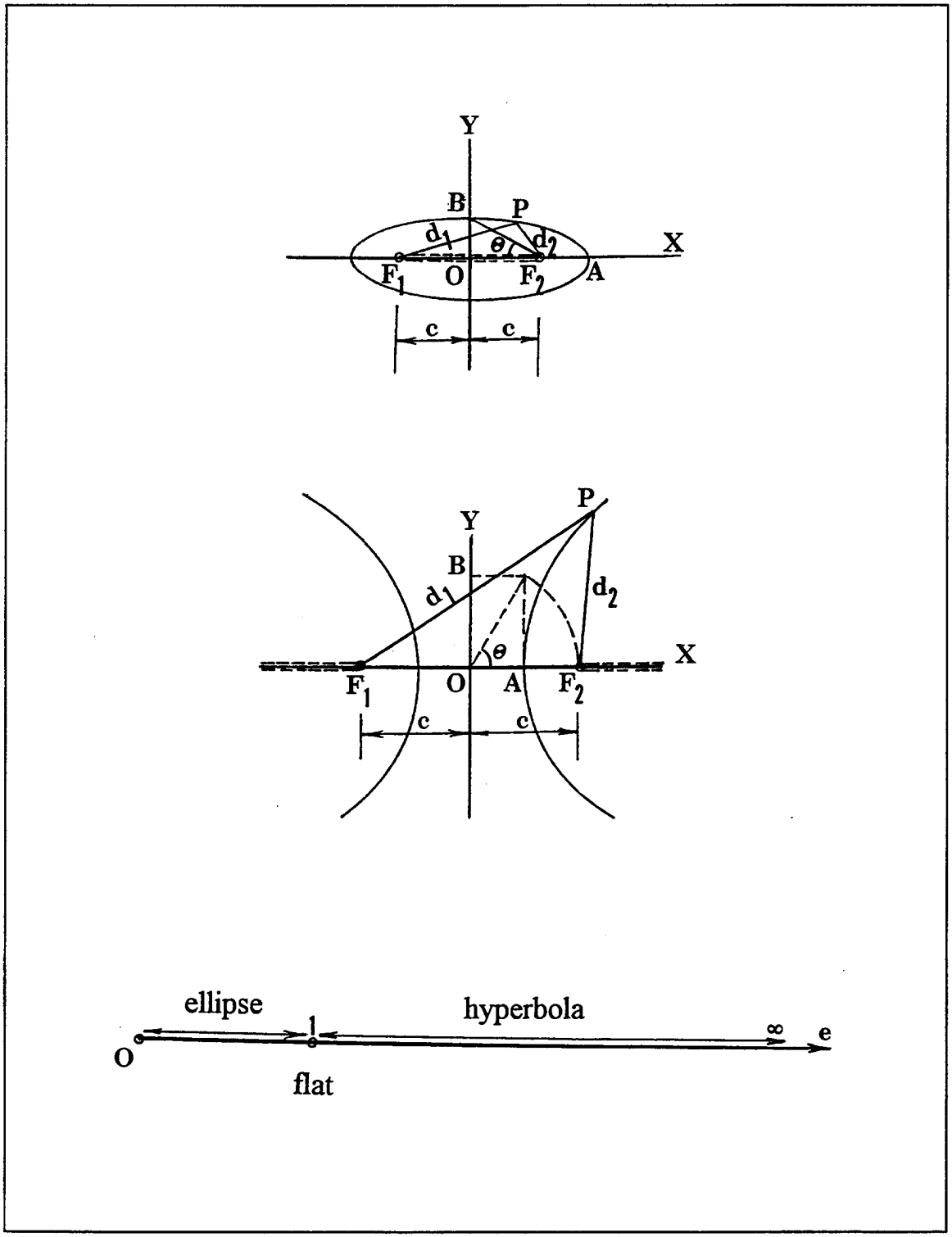

Figure 4. Eccentricity of conics: (a) Ellipse, (b) Hyperbola, and (c) Summary

Hyperbola

Figure 4b shows a general hyperbola with equation:

$$\frac{x^2}{s^2} - \frac{y^2}{t^2} = 1 \tag{5}$$

where s and t are the transverse and the conjugate semiaxes, respectively.

Points P on the hyperbola have the property that the absolute value of the difference between the distances from P to the foci (F_1 and F_2) is constant. The value of the constant is apparent when the end A of the transverse semiaxis is considered:

$$|d_1 - d_2| = 2s \tag{6}$$

Consideration of the end B of the conjugate semiaxis leads to an expression for the focal distance c:

$$c = \sqrt{s^2 + t^2} \tag{7}$$

where $c > s$.

The eccentricity (flatness) of the hyperbola is defined as:

$$e = \frac{c}{s} = \sec\theta \geq 1 \tag{8}$$

The completely flat hyperbola is the discontinuous real axis given by $|x| \geq c$, for which $e = 1$, and the completely upright hyperbola tends to the y-axis, for which $e \to \infty$.

Figure 4c summarizes the classification of the conics according to their eccentricity.

Laminar Flow Through Fundamental Aperture at Boundary of Half-Plane

Consider a plane (of infinite extension) divided in two by a straight and rigid boundary with an aperture of size 2 length units centered at the origin of cartesian coordinates, as shown in Figure 5. The two-dimensional laminar flow through this fundamental aperture is conveniently described in terms of potential theory (de Béjar and Hall 1994).

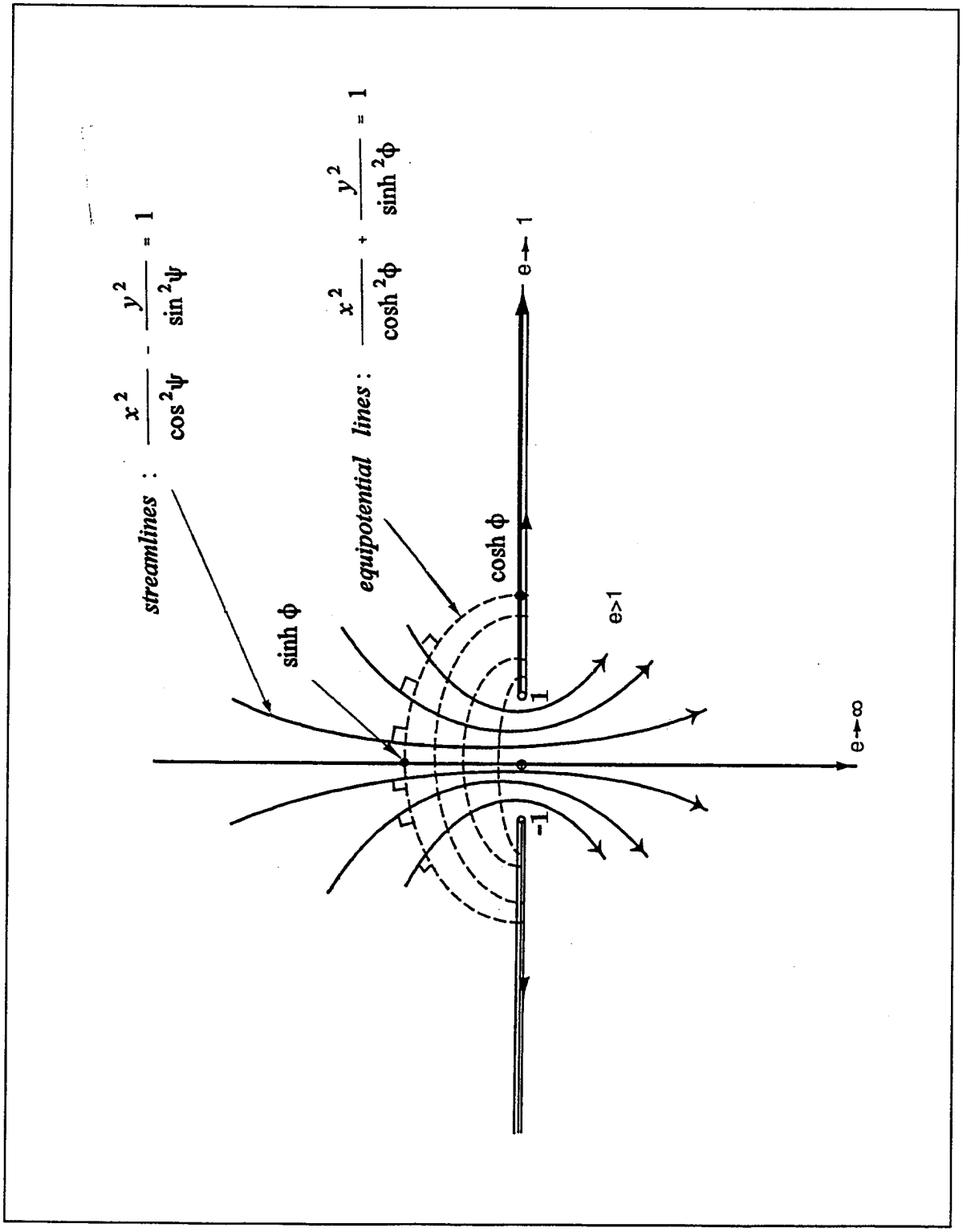

Figure 5. Two-dimensional laminar flow through fundamental aperture

The complex potential in the plane of flow is defined as:

$$F(Z) = \phi(x,y) + i \cdot \psi(x,y) \tag{9}$$

where

$\phi(x, y)$ = potential function (Lamb 1945, Prandtl and Tietjens 1957)

$\psi(x, y)$ = corresponding streamline function

Z = general complex variable

i = imaginary unit

The following complex potential proves to satisfy all boundary conditions of the problem and therefore renders its solution:

$$F(Z) = \cosh^{-1} Z = \ln (Z + \sqrt{Z^2 - 1}) \tag{10}$$

Putting Equation 9 into Equation 10, a system of two real equations is obtained:

$$\begin{aligned} e^{2\phi} \cdot \cos 2\psi - 2\, e^{\phi} \cdot (x \cos\psi - y \sin\psi) + 1 &= 0 \\ e^{2\phi} \cdot \sin 2\psi - 2\, e^{\phi} \cdot (x \sin\psi + y \cos\psi) &= 0 \end{aligned} \tag{11}$$

Elimination of $\phi(x, y)$ in Equations 11 leads to the following geometrical locus, after some algebraic manipulations:

$$\frac{x^2}{\cos^2\psi} - \frac{y^2}{\sin^2\psi} = 1 \tag{12}$$

which defines a family of confocal hyperbolas: the streamlines. In fact, the focal distance for each individual hyperbola is given by Equation 7:

$$c = \sqrt{\cos^2\psi + \sin^2\psi} = 1 \quad (\textit{independent of } \psi) \tag{13}$$

Therefore, the ends of the aperture are the foci for the whole family of hyperbolic streamlines. The eccentricity of each streamline is determined by the specific value of ψ and is given by Equation 8 as $e = \sec\psi \geq 1$.

The corresponding equipotential lines may be obtained by eliminating ψ (x, y) in Equations 11, leading to:

$$\frac{x^2}{\cosh^2 \phi} + \frac{y^2}{\sinh^2 \phi} = 1 \qquad (14)$$

which defines a family of confocal ellipses.

The focal distance for each individual ellipse is given by Equation 3:

$$c = \sqrt{\cosh^2 \phi - \sinh^2 \phi} = 1 \quad (\textit{independent of } \phi) \qquad (15)$$

Therefore, the ends of the aperture are also the foci for the whole family of elliptical equipotential lines which, together with the streamlines, define a network of confocal orthogonal conics. The eccentricity of each equipotential line is determined by the specific value of ϕ and is given by Equation 4 as $e = \text{sech } \phi \leq 1$.

Laminar Flow Through Finite Aperture at Boundary of Half-Plane

Similarly, considering the two-dimensional laminar flow through a finite aperture of size 2a within a straight and rigid boundary dividing in two the plane of the flow leads to a network of confocal orthogonal elliptic equipotential lines and hyperbolic streamlines, as Figure 6 shows.

The conforming complex potential is now given by:

$$F(Z) = K_d \cdot \cosh^{-1} \frac{Z}{a} = K_d \cdot \ln \left(\frac{Z + \sqrt{Z^2 - a^2}}{a} \right) \qquad (16)$$

where K_d is a constant with appropriate dimensions [length^2/time] to be determined from the actual flow velocity measured at a reference point during the experiments on the physical model.

With the definitions $\phi'(x, y) = \phi(x, y)/ K_d$ and $\psi'(x, y) = \psi(x, y)/ K_d$, the family of streamlines is given by the hyperbolas:

$$\frac{x^2}{a^2 \cdot \cos^2 \psi'} - \frac{y^2}{a^2 \cdot \sin^2 \psi'} = 1 \qquad (17)$$

and the family of equipotential lines is given by the ellipses:

$$\frac{x^2}{a^2 \cdot \cosh^2 \phi'} + \frac{y^2}{a^2 \cdot \sinh^2 \phi'} = 1 \qquad (18)$$

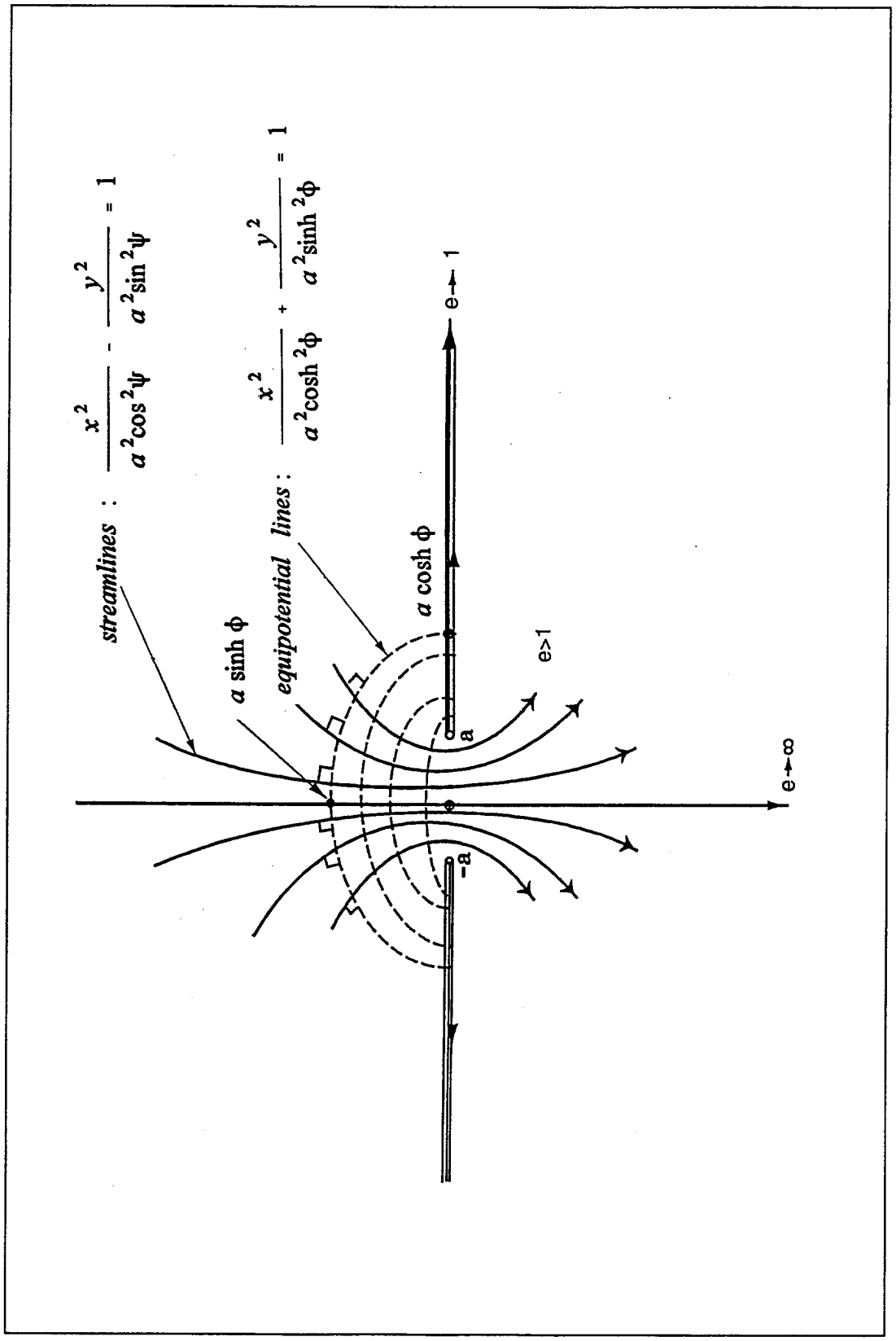

Figure 6. Two-dimensional laminar flow through finite aperture

The common foci for this network of conics are located at the ends of the finite aperture (i.e., $x = \pm a$). The eccentricity of the streamlines is given by $e = \sec \psi' \geq 1$, and the eccentricity of the equipotential lines is given by $e = \operatorname{sech} \phi' \leq 1$.

Mass Flux Through Finite Aperture

The mass flux through a finite aperture of size 2a and unit depth equals, by continuity arguments, the mass flux through the upper half of an arbitrarily selected equipotential line of length, say, Λ (Figure 6). This flux is given by:

$$q = 2\rho \int_{\Lambda} |\{\omega\}| \, d\Lambda \tag{19}$$

where $\{\omega\} = u + i \cdot v$ is the complex velocity field.

The complex conjugate velocity field is given by:

$$\{\omega\}^* = F'(Z) = K_d \cdot \frac{d}{dZ} \left[\cosh^{-1} \frac{Z}{a} \right] \tag{20}$$

Equating real and imaginary parts of Equation 20 yields a system of two real equations for the components u and v of the velocity field:

$$u^2 - v^2 = \frac{x^2 - y^2 - a^2}{(x^2 - y^2 - a^2)^2 + 4x^2y^2} \cdot K_d^2 \tag{21a}$$

$$uv = \frac{xy}{(x^2 - y^2 - a^2)^2 + 4x^2y^2} \cdot K_d^2 \tag{21b}$$

Since $|\{\omega\}|^2 = u^2 + v^2$, the integrand in Equation 19 is obtained as:

$$|\{\omega\}| = \frac{K_d}{\{(x^2 - y^2 - a^2)^2 + 4x^2y^2\}^{\frac{1}{4}}} \tag{22}$$

and the arc length may be obtained by implicit differentiation of Equation 18 as:

$$d\Lambda = \sqrt{1 + \tanh^2\phi' \cdot \left(\frac{a^2}{y^2} \sinh^2\phi' - 1\right)} \, dx \tag{23}$$

Substitution in Equation 19 gives an expression for the flux:

$$q = 2\rho \cdot K_d \cdot sech\,\phi' \int_0^{a\cosh\phi'} \frac{\sqrt{\frac{a^2\cosh^4\phi' - x^2}{a^2\cosh^2\phi' - x^2}}\,dx}{a\cdot([(1+\frac{x}{a})^2 + (\frac{y}{a})^2]\cdot[(1-\frac{x}{a})^2 + (\frac{y}{a})^2])^{\frac{1}{4}}} \qquad (24)$$

$$= \pi\rho \cdot K_d$$

which is independent of both ϕ' and a.

Approach Velocity

Figure 7 shows schematically a plan view of the velocity field on the upstream surroundings of the gate. The average flow velocity through the aperture may be estimated from:

$$V = \frac{\pi \cdot K_d}{2\,a\,\alpha} = \frac{\pi \cdot K_d}{2\,a}\cdot\left(\frac{1}{1 - 0.389\,\delta}\right) \qquad (25)$$

where α is the coefficient of contraction, and $\delta = z/h$ is the nondimensional vertical coordinate of the layer being considered, with origin at the gate hinge and positive upwards, normalized with respect to the water depth at the gate hinge: h (i.e., $\delta \in (0,1)$). Equation 25 implies linear variation of the coefficient of contraction from $\alpha = 1$, at the gate hinge, to its experimental value as obtained by Kirchhoff, $\alpha = 0.61$ (Lamb 1945, Prandtl and Tietjens 1957), at the gate ridge.

Joukowski's Transformation

Consider the conformal mapping of circles $x^2 + y^2 = R^2$ in the complex Z-plane into the complex ζ-plane ($\zeta = \xi + i \cdot \eta$) under the Joukowski's transformation:

$$\zeta = Z + \frac{b^2}{4Z}, \quad b > 0 \qquad (26)$$

A set of two real equations is obtained:

$$x = \frac{\xi}{1 + \frac{b^2}{4R^2}} \qquad (27a)$$

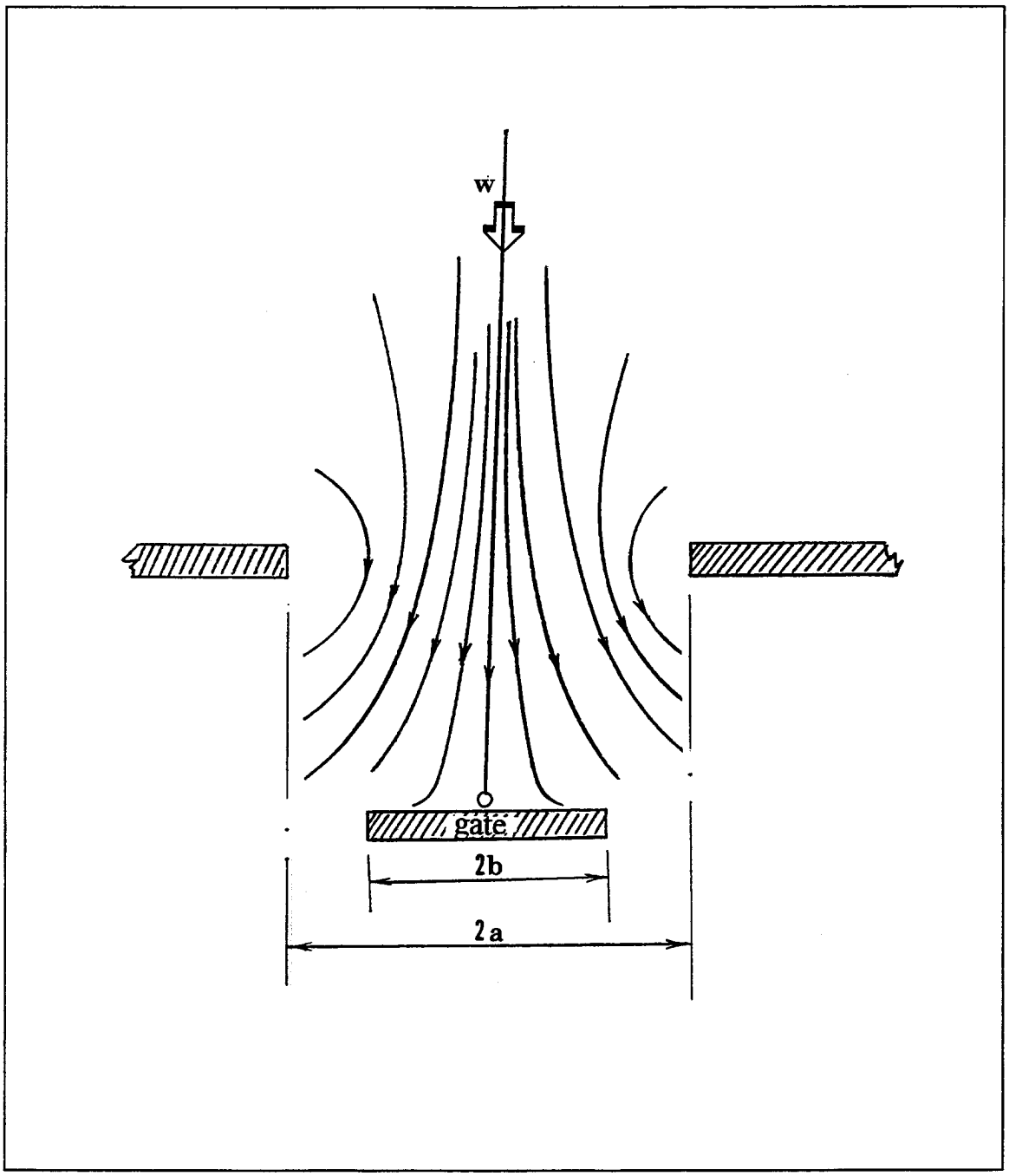

Figure 7. Velocity field on upstream surroundings of gate

$$y = \frac{\eta}{1 - \frac{b^2}{4R^2}} \tag{27b}$$

If Equations 27 are inserted in the original circle equation, the following family of ellipses is obtained as a result of the transformation:

$$\frac{\xi^2}{(R + \frac{b^2}{4R})^2} + \frac{\eta^2}{(R - \frac{b^2}{4R})^2} = 1 \tag{28}$$

The focal distance for these ellipses is given by Equation 3:

$$\xi_0^2 = (R + \frac{b^2}{4R})^2 - (R - \frac{b^2}{4R})^2 = b^2 \tag{29}$$

or $\xi_0 = b$ (independent of R!).

Therefore, Joukowski's transformation maps concentric circles $x^2 + y^2 = R^2$, in the Z-plane, into confocal ellipses in the ζ-plane, with eccentricities given by:

$$e = \frac{2}{\frac{2R}{a} + \frac{b}{2R}} \tag{30}$$

Note, in particular, that the circle $| Z | = b/2$ transforms into the flat focal segment F_1F_2 (e =1), as Figure 8a shows. On the other hand, a circle on the open disk $| Z | < b/2$ maps into a corresponding ellipse in the ζ-plane, in such a way that the disk maps into the whole slit ζ-plane (i.e., the ζ-plane without F_1F_2). The semi-infinite open annulus $| Z | > b/2$ again maps into the whole slit ζ-plane, as Figure 8b shows.

Velocity Field on Upstream Face of Gate

Applying the sequence of complex-plane conformal mappings described in Figure 9, i.e., inverse Joukowski's transform followed by a quadrant rotation and a direct Joukowski's transform (Greenberg 1978), one arrives at the simple hydrodynamic problem involving flow parallel to a plate, with obvious solution. Transforming back to the original complex plane, the components of the velocity field are obtained from the following set of simultaneous equations:

$$u^2 - v^2 = -V^2 \cdot (1 + \frac{b^2 \cdot (x^2 - y^2 - b^2)}{(x^2 - y^2 - b^2)^2 + 4x^2y^2}) \tag{31a}$$

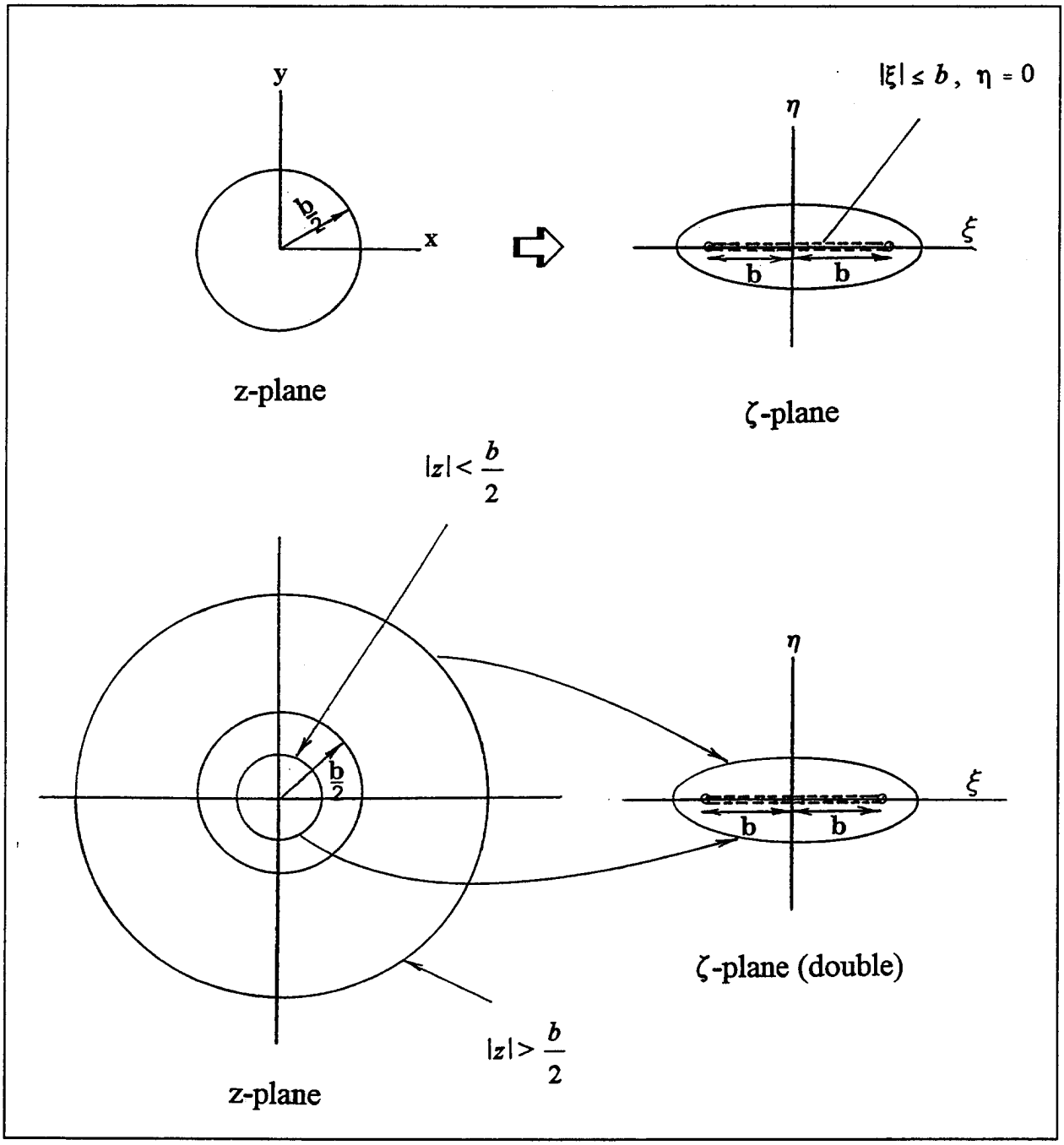

Figure 8. Joukowski's transformation in the complex plane applied to (a) the circle |z| = b/2, and (b) a circle either internal or external to the circle |z| = b/2

$$uv = -V^2 \cdot b^2 \cdot \frac{xy}{(x^2 - y^2 - b^2)^2 + 4x^2y^2} \qquad (31b)$$

When evaluated on the vertical projection of the upstream face of the gate ($|x| \le b$, $y=0$), Equations 31 give:

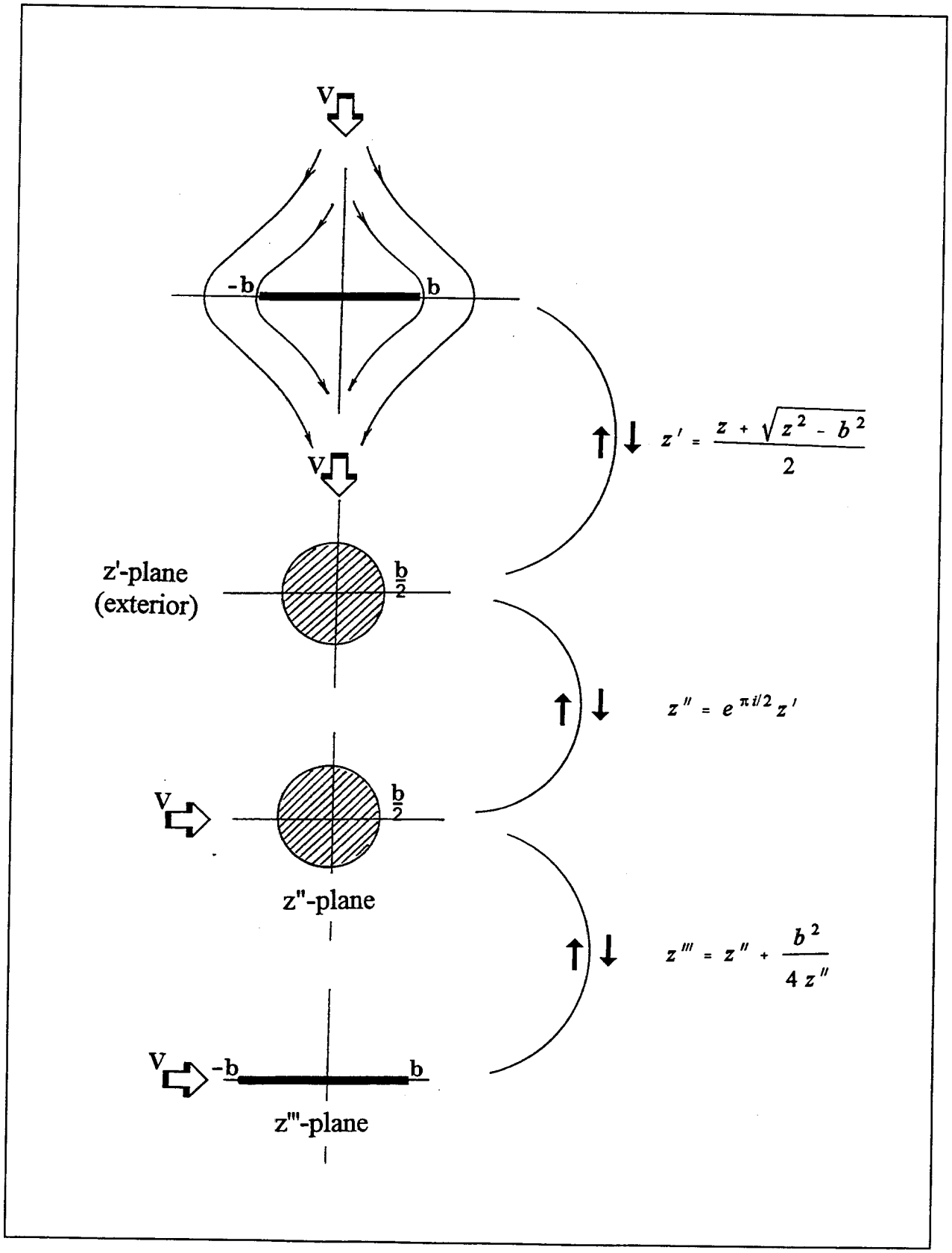

Figure 9. Sequence of complex transformations

$$\begin{cases} u = \dfrac{Vx}{\sqrt{b^2 - x^2}}, & |x|<b \\ v = 0 \end{cases} \tag{32}$$

Inserting Equation 25 in Equation 32 gives:

$$u = \left(\frac{\pi K_d}{2a}\right) \cdot \frac{1}{1 - 0.389\,\delta} \cdot \frac{x}{\sqrt{b^2 - x^2}}, \quad |x|<b \tag{33}$$

This velocity field is schematically represented in Figure 10. Notice that u vanishes for x = 0; therefore, the center line of the upstream face of the gate is effectively a stagnation line.

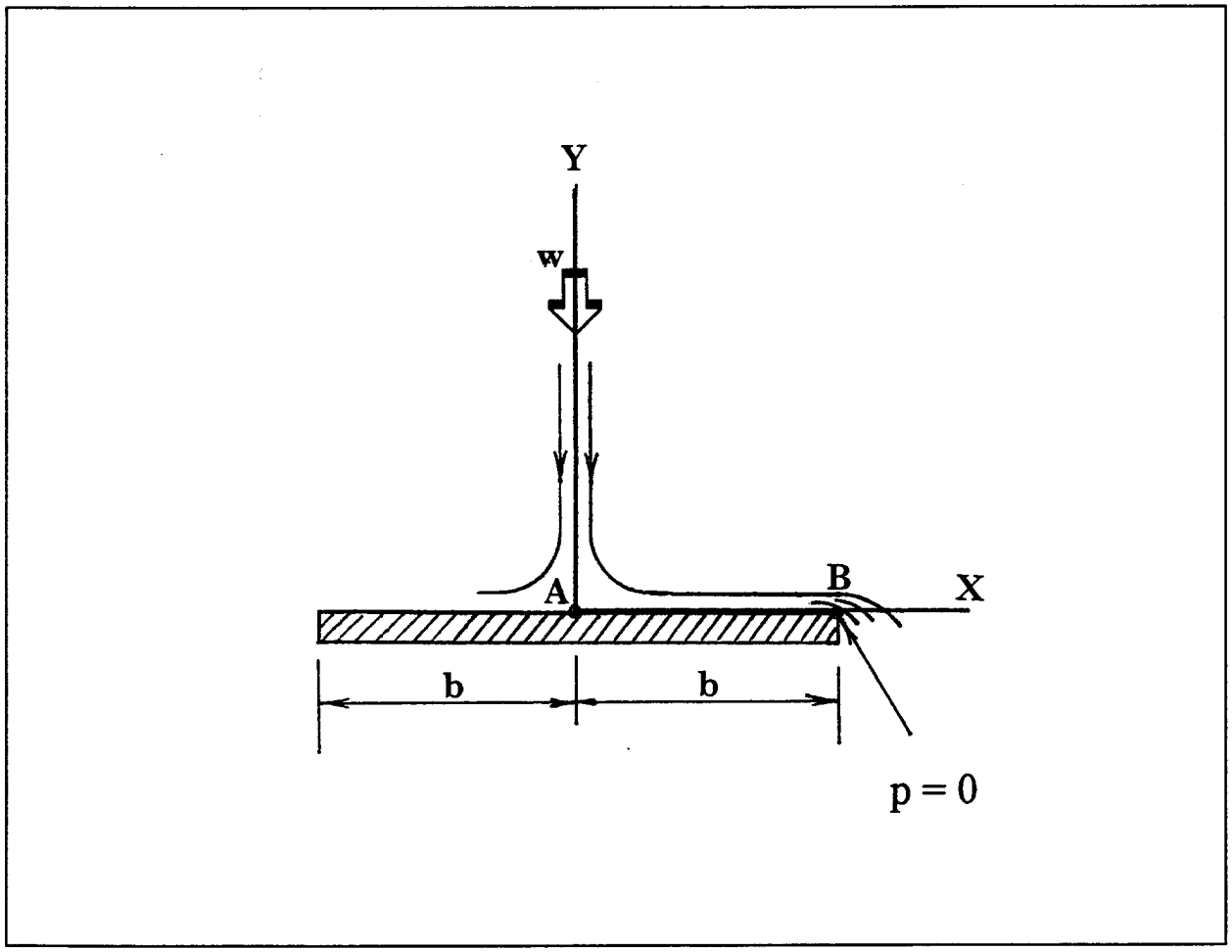

Figure 10. Velocity field on upstream face of gate

Estimation of Hydrodynamic Pressure Field on Gate

The steady-state component of the hydrodynamic pressure field on the gate is conveniently estimated from Bernoulli's energy-balance equation for the streamline along the y-axis in Figure 10, from $y \to \infty$ to the stagnation point A, followed by the same formulation for points internal to the segment AB ($|x|<b$).

For the y-axis streamline, between a far away point and point A, one has:

$$p_A = \frac{\rho V^2}{2} \tag{34}$$

Using Equation 34, one has for points on segment AB:

$$p(x) = \frac{\rho}{2} \cdot (V^2 - u^2) \tag{35a}$$

or, normalizing to obtain a nondimensional expression:

$$\frac{p(\beta)}{(\frac{\rho V^2}{2})} = 1 + \frac{1}{1 - (\frac{1}{\beta})^2}, \quad |\beta|<1 \tag{35b}$$

where $\beta = x/b$.

This pressure field vanishes for $\beta_0 = 1/\sqrt{2}$, and becomes suctional toward the gate edges, its magnitude increasing without limit at B. This happens because the magnitude of the velocity in Equation 33 also grows unboundedly as x approaches b. On account of the viscosity in a real fluid, the flow velocity and the associated suction will only attain a bounded magnitude in the regions of the gate toward the edges. Also, in an actual situation, the hydrodynamic pressure at the very edge B must be zero, as indicated graphically in Figure 10. In an attempt to represent these effects in the model, the hydrodynamic suction is allowed to grow to a certain value and then is assumed to approach its boundary value at B ($p_B = 0$) in a linear fashion (see Figure 11). The equivalent normalized distance $\Delta\beta$ that defines the hydrodynamic pressure distribution is identified below by experimental analysis.

Hydrodynamic Line Force on Vertical Projection of Gate

Integrating the hydrodynamic pressure field over the gate width, one obtains an expression for the resultant hydrodynamic force on the vertical projection of the gate, per unit length of height:

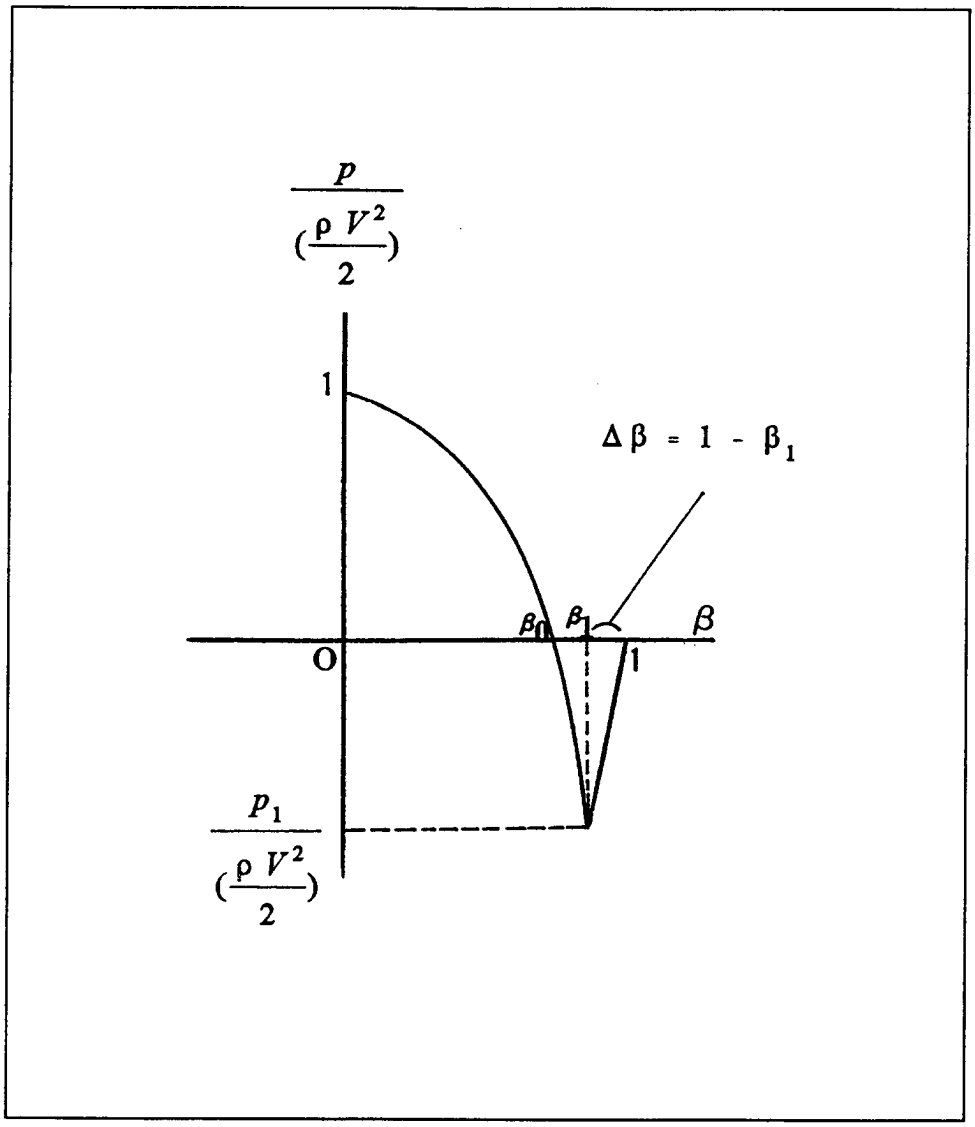

Figure 11. Hydrodynamic pressure on the right-half upstream face of gate

$$f_H = \int_{-\beta_1}^{+\beta_1} \frac{\rho V^2}{2} \cdot (1 + \frac{\beta^2}{\beta^2 - 1}) d\beta + \frac{\rho V^2}{2} \cdot (1 + \frac{\beta_1^2}{\beta_1^2 - 1}) \cdot (1 - \beta_1) \quad (36)$$

or, normalizing to obtain a nondimensional expression:

$$\frac{f_H}{(\frac{\rho V^2}{2}) \cdot b} = 4\beta_1 - \ln\frac{1 + \beta_1}{1 - \beta_1} - \frac{2\beta_1^2 - 1}{1 + \beta_1}, \quad \beta_1 \geq \beta_0 \quad (37)$$

or, in terms of the equivalent normalized distance $\Delta\beta$:

$$\frac{f_H}{(\frac{\rho V^2}{2}) \cdot b} = \chi(\Delta\beta) = \frac{8(1 - \Delta\beta) - 1}{1 + (1 - \Delta\beta)} - \ln(\frac{2}{\Delta\beta} - 1) \quad (38)$$

Hydrodynamic Resultant Force on Vertical Projection of Gate

Integrating the hydrodynamic line force in Equation 38, the hydrodynamic resultant force on the vertical projection of the gate is obtained as:

$$F_H = \frac{\rho b}{2} \cdot \chi(\Delta\beta) \cdot \int_0^h V^2 \, dz \quad (39)$$

or, normalizing to obtain a nondimensional expression:

$$\frac{F_H}{\rho K_d^2} = \frac{\pi}{2} \cdot (\frac{\pi}{2} + 1) \cdot \frac{Ag}{(2a)^2} \cdot \chi(\Delta\beta) \cdot \sin\theta \quad (40)$$

where

Ag = area of the upstream face of the gate

θ = gate elevation (Figure 12)

The location of the corresponding pressure center is given by:

$$\bar{z} = \frac{1}{F_H} \cdot \int_0^h z \cdot (f_H \, dz) \quad (41a)$$

or, after normalizing:

$$\bar{\delta} = (\frac{h}{F_H}) \cdot \int_0^1 (\frac{\rho V^2}{2}) b \cdot \chi(\Delta\beta) \, \delta \, d\delta \quad (41b)$$

which leads to:

$$\bar{z} = 0.58 \, h \quad (42)$$

which is a fixed value for a given gate elevation (θ).

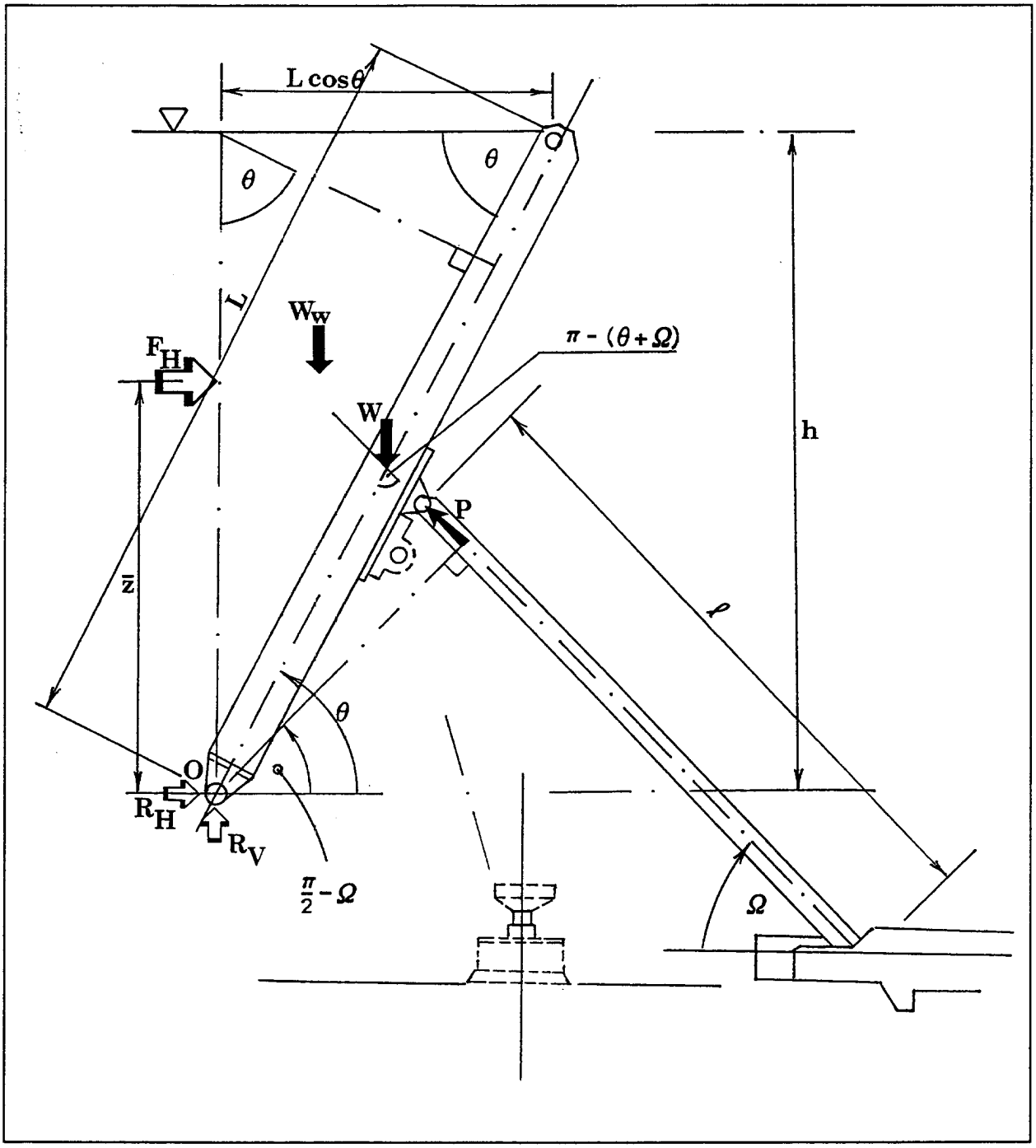

Figure 12. Equilibrium of forces on gate

3 Application of Theory

Reactive Thrust at Support Shaft

Figure 12 shows the free-body diagram for the gate at elevation θ, subjected to both static and hydrodynamic loads. W in the figure is the dry weight of the gate, whereas W_w is the weight of the water supported by the gate. F_H is the resultant hydrodynamic force on the vertical projection of the gate acting at the pressure center defined by $\bar{z}$. P is the resultant axial load in the support shaft (prop reaction), acting at an inclination Ω. R_H and R_V are the horizontal and vertical components, respectively, of the resultant reaction at the support hinge of the gate.

The prop reaction, P, is easily expressed in terms of F_H, by considering the rotational equilibrium of the gate:

$$P = F_H \cdot \left(\frac{\bar{z}}{d}\right) + \frac{L}{d} \cdot \cos\theta \cdot \left(\frac{W_w}{3} + \frac{W}{2}\right) \tag{43}$$

Once the prop reaction is known, the components of hinge reaction R_H and R_V may be conveniently obtained from the translational equilibrium of the gate:

$$R_H = P\cos\Omega - F_H \tag{44}$$

$$R_v = W + W_w - P\sin\Omega \tag{45}$$

and the function $\chi(\Delta\beta)$ can be identified, if desired, by inserting Equation 40 into Equation 43:

$$\chi(\Delta\beta) = \frac{P\sin(\theta + \Omega) - (W + W_w)\cos\theta}{4.7\rho K_d^2 \frac{A\,g}{(2a)^2}\sin^2\theta} \tag{46}$$

The difficulty is precisely that P depends on the hydrodynamic resultant F_H, which in turn depends on Δβ. This closed cycle of cause and effect is broken through experimental analysis. Statistical characterization of experimental

records of prop reaction (P) in a small-scale physical model conveniently define the hydraulic forces and allow their prediction for the prototype gate.

Second-Moment Statistical Characterization of Response Parameters

Let the total prop reaction, P, consist of two components: (1) P_s, the hydrostatic component, and (2) P_H, the reaction to the hydrodynamic force on the gate, F_H (Naudascher 1991). Thus, from Equation 43, one has the hydrostatic component:

$$P_s = \frac{L}{d} \cos\theta \left(\frac{W}{2} + \frac{W_w}{3} \right) \tag{47}$$

which is taken as deterministic and is readily computed.

Also from Equation 43, one has for the hydrodynamic component:

$$P_H = \frac{\overline{z}}{d} \cdot F_H \tag{48a}$$

or

$$P_H = 1.16 \frac{\sin\theta}{\sin(\theta + \Omega)} \cdot F_H \tag{48b}$$

which may be written as:

$$F_H = R(\theta) \cdot P_H \tag{48c}$$

where

$$R(\theta) \sim \sin\frac{2\pi}{3} \cdot \frac{\sin(\theta + \Omega)}{\sin\theta} \tag{48d}$$

Figure 13 shows the hydrodynamic equilibrium of forces on the gate. Notice that, in general, the reaction at the support hinge, R, pulls the gate with a downward vertical component.

The transfer factor in Equation 48d, $R(\theta)$, does not vary much with either the prop inclination (Ω) or the gate elevation (θ) for $\theta > 30°$, as Figure 14a illustrates. The neighborhood of $\theta = 60°$ is expanded in Figure 14b. Notice that for a prop inclination $\Omega = 45°$ and gate elevation $\theta \sim 60°$, $P_H \sim F_H$.

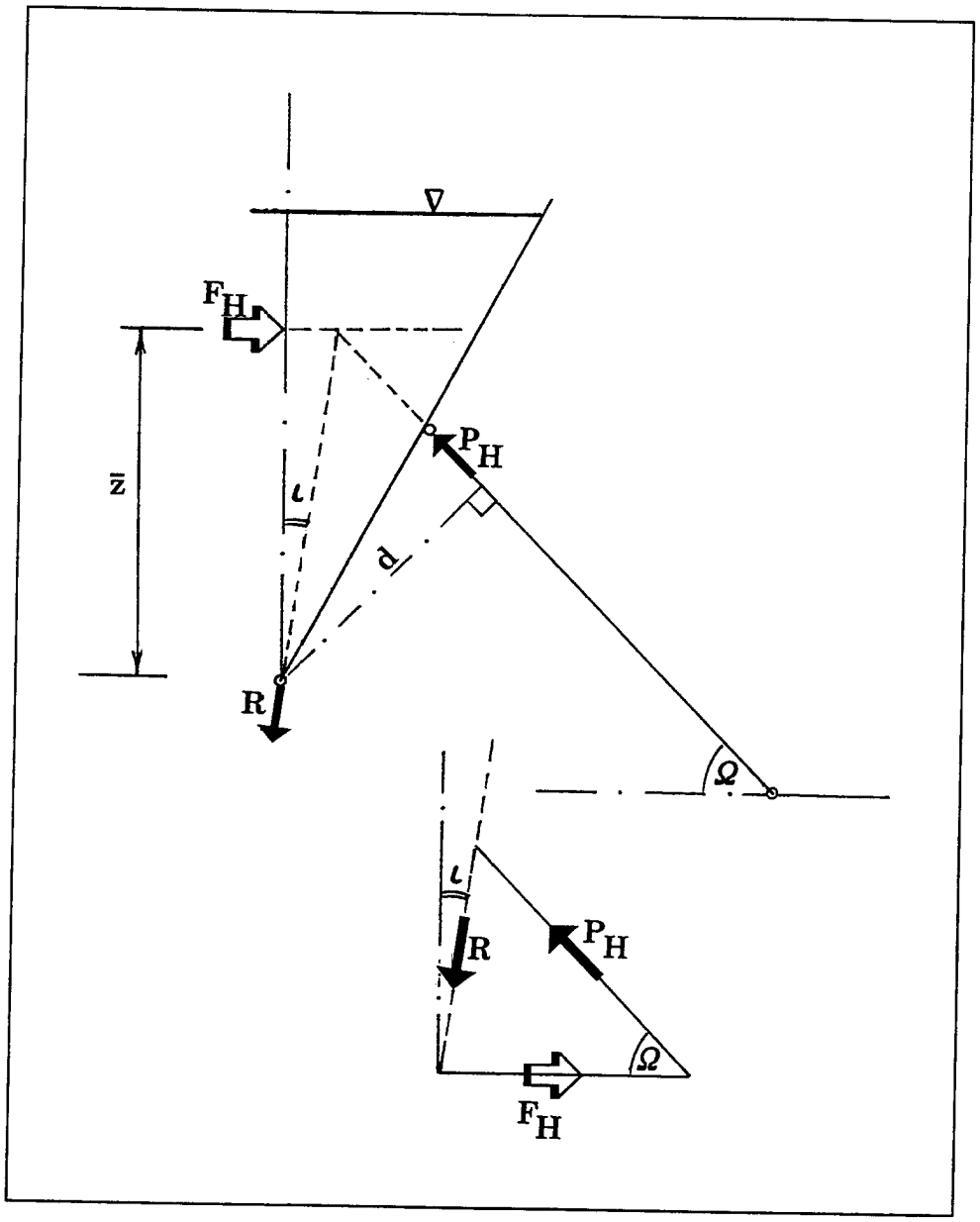

Figure 13. Hydrodynamic equilibrium of forces on gate

In general, the expected value, the standard deviation, and the coefficient of variation of the hydraulic force on the gate are respectively given by:

$$E(F_H) = R(\theta) \cdot E(P_H) \tag{49a}$$

$$\sigma_{F_H} = R(\theta) \cdot \sigma_{P_H} \tag{49b}$$

$$\nu_{F_H} = \nu_{P_H} \tag{49c}$$

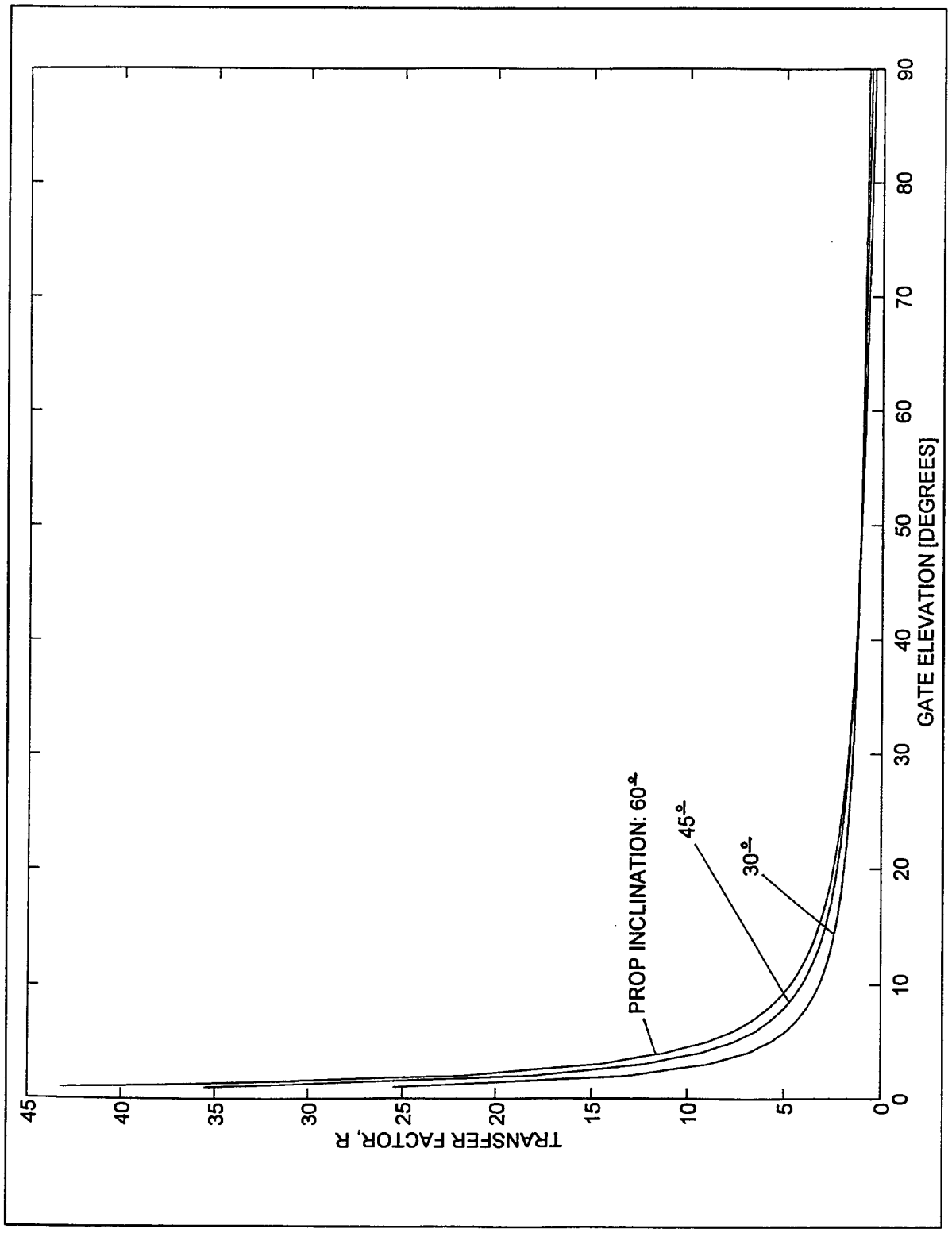

Figure 14a. Variation of transfer factor, R(θ), with gate elevation (θ = 0...90°)

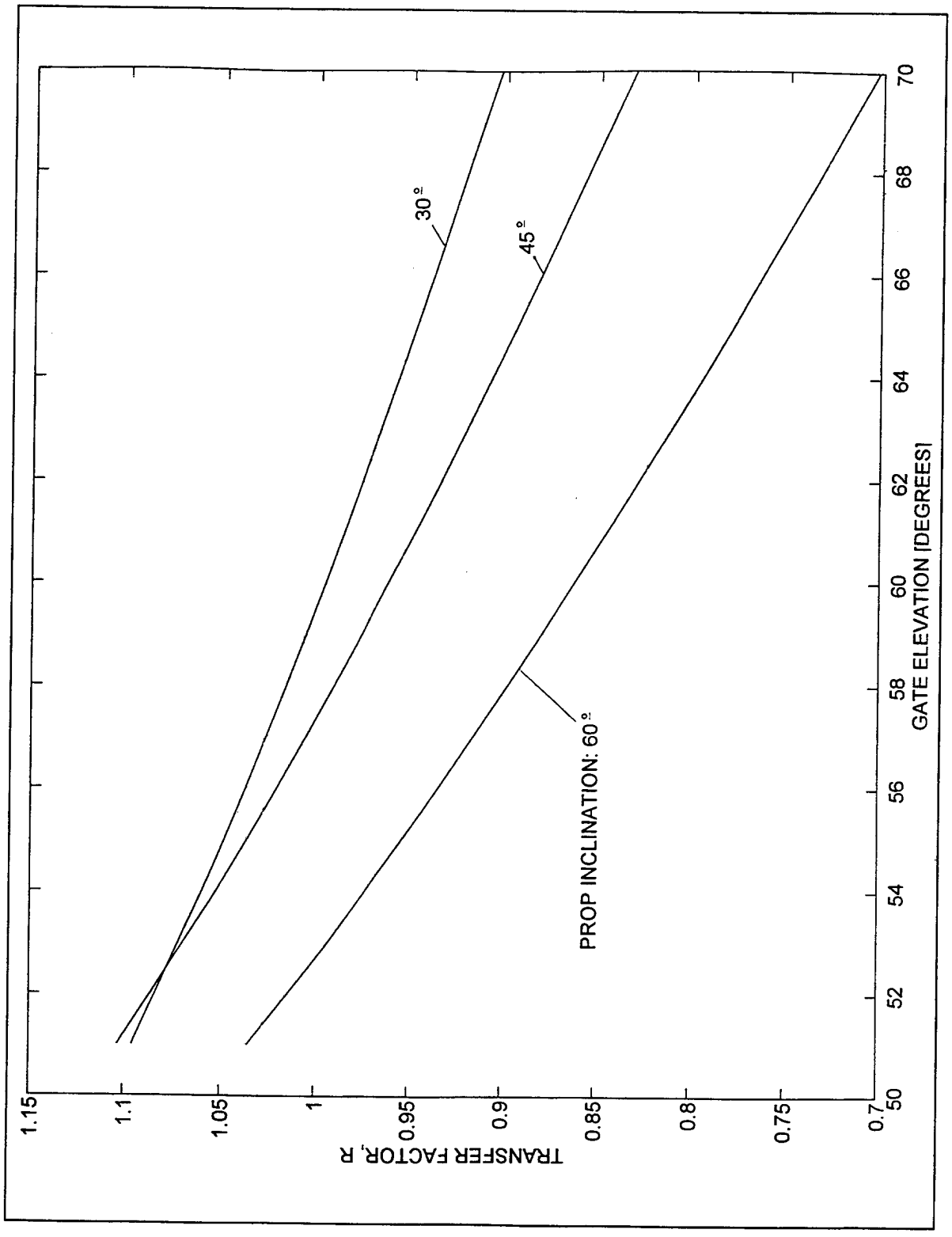

Figure 14b. Variation of transfer factr, R(θ), with gate elevation (θ = 50°...70°)

in terms of the corresponding quantities for the prop reaction.

Previous experience with multiple similar records (de Béjar 1995; de Béjar and Hall 1995a,b; Fletcher and de Béjar 1995) suggests that, for all practical purposes, the distribution of the peaks of P_H is approximately normal. Therefore, the statement can be made that, with ~ 97 percent confidence, the upper and lower bounds to the design hydrodynamic load on the gate may be taken as:

$$F_H^* = E(F_H) \pm 3 \cdot \sigma_{F_H} \tag{50}$$

applied at the hydrodynamic pressure center:

$$\bar{z} = 0.58\,h \tag{51}$$

If the physical model is designed according to Froude's law with fluid-density scaling $\lambda_\rho = 1$, then the upper and lower bounds to the magnitude of the hydrodynamic force on the prototype, in terms of the same force in the model, are given by (Novak and Cabelka 1981):

$$F^*_{H,PROTOTYPE} = \lambda_L^3 \cdot F^*_{H,MODEL} \tag{52}$$

where λ_L is the scaling factor for length, and the hydrodynamic forces are applied at the homologous pressure centers (δ).

The second-moment characterization of the function $\chi(\Delta\beta)$ is readily obtained from Equation 40 (Benjamin and Cornell 1970):

$$E[\chi(\Delta\beta)] = \frac{E(F_H)}{\rho K_d^2 \cdot \frac{\pi}{2} \cdot (\frac{\pi}{2} + 1) \cdot \frac{Ag}{(2a)^2} \sin\theta} \tag{53a}$$

$$\sigma_\chi = \frac{\sigma_{F_H}}{\rho K_d^2 \cdot \frac{\pi}{2} \cdot (\frac{\pi}{2} + 1) \cdot \frac{Ag}{(2a)^2} \sin\theta} \tag{53b}$$

$$\nu_\chi = \nu_{F_H} = \nu_{P_H} = \nu_{(\frac{P_H}{P_s})} \tag{53c}$$

Given an experimental record for P_H in a physical model, by assuming the record to be part of a sample of an ergodic process, the moments of P_H are estimated from the average [~ $E(P_H)$] and the area under the power spectral density function [~ σ_{PH}^2] (Bendat and Piersol 1993, Crandall and Mark 1963). Then, the analysis proceeds by evaluating Equations 49 through Equations 53.

Alternately, if from past experience, the expected value and the coefficient of variation of the ratio P_H/P_s may be assumed, then the moments of P_H may be estimated by:

$$E(P_H) = E(P_H/P_s) \cdot P_s \tag{54a}$$

$$\sigma_{P_H} = \nu(P_H/P_s) \cdot E(P_H) \tag{54b}$$

and the analysis proceeds by evaluating Equations 49 through Equations 53, as above.

4 Verification of Theory

Approximate Experimental Verification

The mathematical model for the resultant hydrodynamic force on the gate was approximately verified from experiments on a 1/15-scale physical model of a typical wicket gate for the Olmsted locks-and-dam project. A model gate in closed position ($\theta = 60°$) at the center of a three-gate aperture faced a ridge-level upper pool, with the lower pool below the level of the support hinge (see the example of application below for other characteristics of the physical model).

Under these hydraulic conditions, the velocity of the approaching flow at the surface was measured approximately as 3.048 m/sec (10 fps) at the center of the aperture, from which Equation 25 gives $K_d = 0.072$ m^2/sec. Taking, as a first approximation, $\Delta\beta \sim (1-\beta_0)/2$, Equation 38 gives $\chi(\Delta\beta) \sim 0.609$, and Equation 40 provides an estimate of the resultant hydrodynamic force on the gate as $F_H \sim 27.8$ N. This approximate semitheoretical estimate should be compared with the average of the directly measured experimental value of the same force obtained from Equation 49a, after averaging the records of calibrated strain gages on the model gate shaft:

$$E(F_H) = E(P_H) = 29.15\ N$$

The semitheoretical estimate errs by approximately 5 percent on the unconservative side, but this relatively small error suggests the usefulness of the semitheoretical model for engineering applications.

Example of Application

The procedure for the statistical characterization of response parameters is illustrated with an example of application for the Olmsted locks-and-dam project. Figure 15 shows a typical 30-second record for the total shaft load on a 1/25-scale physical model of a wicket gate at WES, under ridge-level upper pool and lower pool below the level of the support hinge. Figure 16 shows the corresponding power spectral density function. The hydraulic environment is that associated

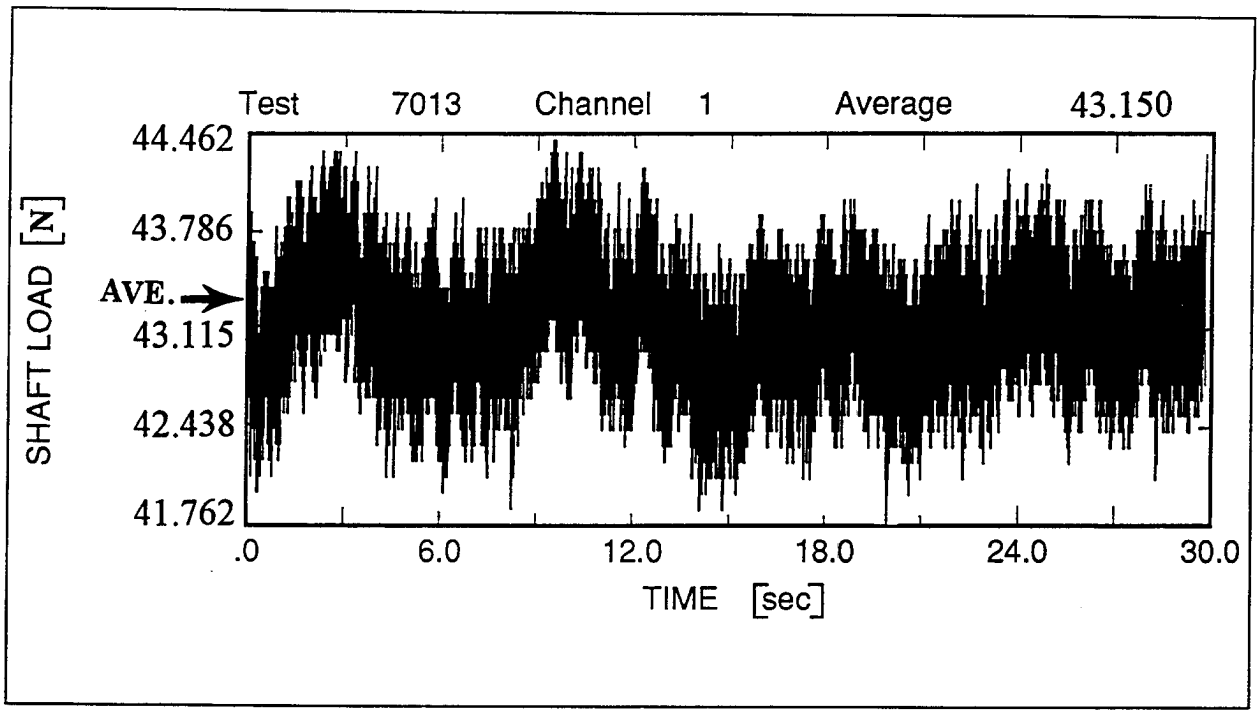

Figure 15. Time history of shaft load response (after Chowdhury, Hall, and Pesantes (1994))

with flow through a three-gate aperture impinging on a single central gate in closed position ($\theta = 60°$). Under these conditions, the flow is observed to be quasi-laminar. Other pertinent quantities for the physical model are:

Aperture size: 370 mm.
Dimensions of the physical model gate: 118mm x 317 mm.
Weight of the physical model gate (W): 10.23 N.

Prop inclination (Ω): 45°.
K_d (identified during the experiment): 0.072 m^2/sec.
Unit weight of water (T = 16 C°): $\gamma_w = 9{,}800$ N/m^3.

Estimation of hydrodynamic force on the prototype gate:

The weight of the water acting directly on the gate is given by:

$$W_w = \frac{1}{4} \cdot \gamma_w \, Ag \, L \, \sin(2\theta) = 25.15 \, N$$

The hydrostatic component of the prop reaction is obtained as:

$$P_s = \frac{2 \cdot \cos 60°}{\sin(60 + 45)°} \cdot \left(\frac{10.23}{2} + \frac{25.15}{3}\right) = 14 \, N,$$

which allows the calculation of the mean value of P_H as:

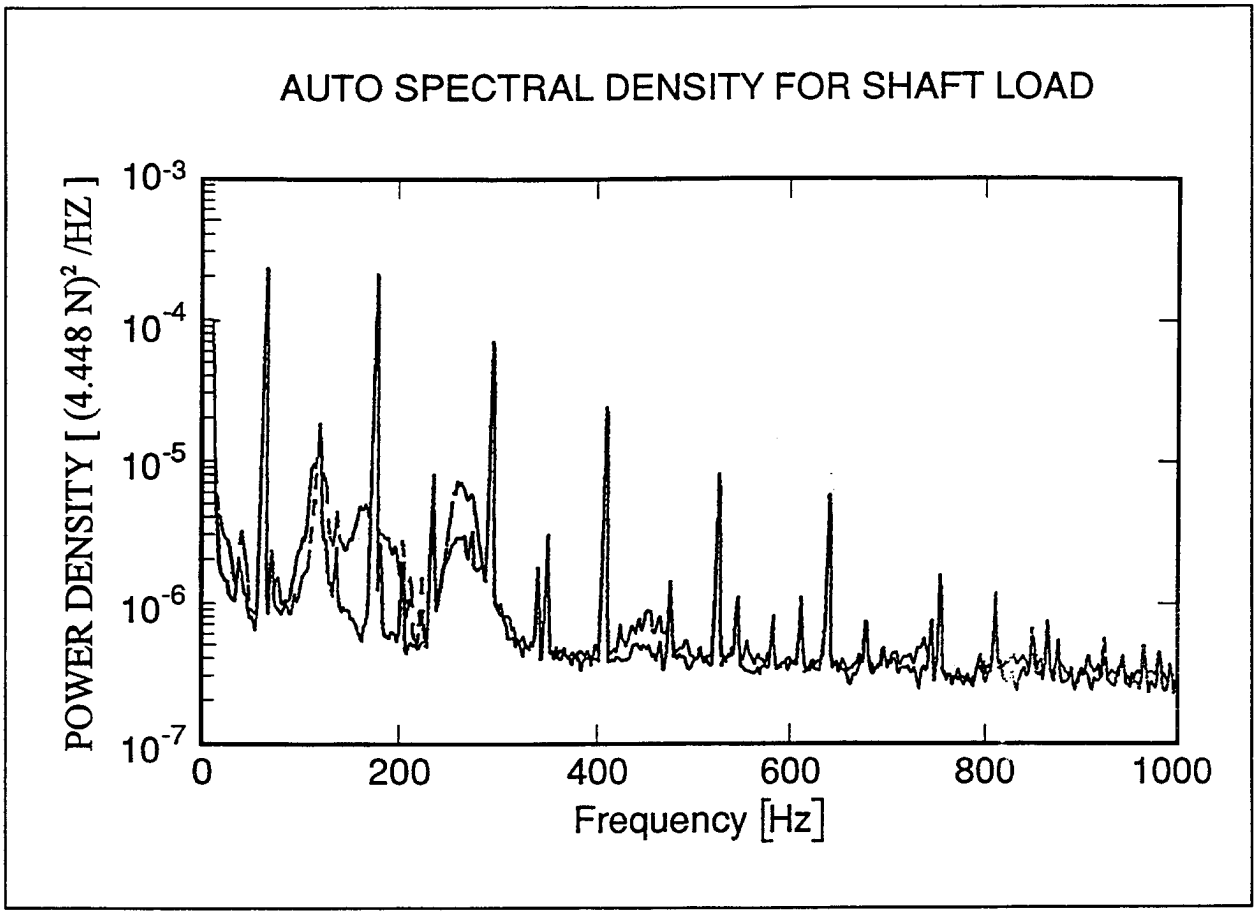

Figure 16. Autospectral density of shaft load (after Chowdhury, Hall, and Pesantes (1994))

$$E(P_H) = E(P) - P_s = 43.15 - 14 = 29.15\,N$$

The variance of the hydrodynamic prop reaction, P_H, is obtained by computing the area under the power spectral density function (Figure 16): $\sigma_{PH}^2 \sim 0.198\ N^2$.

$$\therefore \quad \nu_{P_H} = \frac{\sigma_{P_H}}{E(P_H)} = 0.01$$

From Figure 14b, the transfer factor is obtained as $R(\theta) = 0.96$

Equation 49a gives:

$$E(F_H) = R(\theta) \cdot E(P_H) = 0.96 \cdot 29.15 = 28\,N$$

and Equation 49b gives:

$$\sigma_{F_H} = R(\theta) \cdot \sigma_{P_H} = 0.96 \cdot 0.445 = 0.43\,N$$

The 97 percent confidence range for the resultant hydrodynamic force on the physical-model gate is given by Equation 50:

$$F_H^* = E(F_H) \pm 3 \cdot \sigma_{F_H} = 28 \pm 3 \cdot 0.43 = (26.7\,N,\ 29.3\,N),$$

applied at the pressure center given by Equation 51:

$$\bar{z} = 0.58 \cdot 317 \cdot \sin 60° = 159\ mm$$

For a physical model designed according to Froude's law, with $\lambda_\rho = 1$, the estimate of the 97 percent confidence range for the resultant hydrodynamic force on the prototype gate is given by Equation 52:

$$F_{H_{PROTOTYPE}}^* = 25^3 \cdot (26.7\,N, 29.3\,N) = (417\,kN, 458\,kN)$$

applied at $\bar{z} = 4$m.

5 Conclusions

This investigation has produced a mathematical model that allows an engineering estimate of the hydraulic forces on a prototype wicket gate in operation under the hydraulic environment associated with flow through a three-gate aperture impinging on a single central gate in closed position. This is one of the critical conditions to be considered in the gate design. The model is not valid for other hydraulic environments involving turbulence in the back of the gate.

It is recommended that two basic measurements be taken during the experiments with a small-scale physical model to completely define the theoretical development: (1) the velocity of the approaching flow at a specific point of the reservoir nearby the aperture, and (2) a time-history record of the prop reaction for the gate in operation in closed position. The model predicts sufficiently close bounds for the peak hydraulic forces as to produce reliable designs.

References

Bendat, J. S., and Piersol, A. G. (1993). *Engineering Applications of Correlation and Spectral Analysis, 2nd Ed.* John Wiley, New York, NY.

Benjamin, J. R., and Cornell, C. A. (1970). *Probability, Statistics, and Decision for Civil Engineers.* McGraw-Hill, New York, NY.

Crandall, S. H., and Mark, W. D. (1963). *Random Vibration in Mechanical Systems.* Academic Press, New York, NY.

Chowdhury, M. R., Hall, R. L., and Pesantes, E. (1994). "Flow-induced vibrational test results for a 1:25 flat wicket gate." A report for the U.S. Army Engineer District, Louisville, KY.

de Béjar, L. A. (1995). "Montgomery point lock and dam study; Report 2, Montgomery Point Torque-Tube Gate, A structural model study." Technical Report SL-95-14, U.S. Army Engineer Waterways Experiment Station, Vicksburg, MS.

de Béjar, L. A., and Hall, R. L. (1994). "Modelling quasi-laminar flow-induced pressure fields on hydraulic wickets." *Proc., 65th Shock and Vibration Symposium,* SAVIAC, San Diego, CA., Vol. 2, 295-304.

_____. (1995a). "Montgomery Point Torque-Tube Gate Model: Extreme-value analysis of experimental data." Proc., *66th Shock and Vibration Symposium,* SAVIAC, Biloxi, Mississippi, Vol. 1, 379-389.

_____. (1995b). "White river entrance channel: Montgomery Point Lock and Dam Torque-Tube Gate 1/15-scale model study." Proc., *Corps of Engineers Structural Engineering Conference*, CESEC, San Antonio, Texas.

Fletcher, B. P., and de Béjar, L. A. (1995). "Montgomery Point Lock and Dam Study; Report 1, Hydraulic forces and characteristics acting on spillway gates." Technical Report SL-95-14, U.S. ArmyEngineer Waterways Experiment Station, Vicksburg, MS.

Greenberg, M. D. (1978). *Foundations of Applied Mathematics.* Prentice-Hall, Englewood Cliffs, NJ.

Kreyszig, E. (1988). *Advanced Engineering Mathematics, 6th Ed.* John Wiley, New York, NY.

Lamb, H. (1945). *Hydrodynamics, 6th Ed.* Dover Publications, New York, NY.

March, P. A., and Elder, R. A. (1992). *Review of the 1:25 Scale Hydraulic Model Olmsted Wicket Dam.* USAE, Ohio River Division. Contract No. DACW55-92-0187.

Naudascher, E. (1991). *Hydrodynamic Forces, Volume 3: Hydraulic Structures Design Manual, Hydraulic Design Considerations.* International Association for Hydraulic Research. A.A. Balkema, Rotterdam, Netherlands.

Novak, P., and Cabelka, J. (1981). *Models in Hydraulic Engineering: Physical Principles and Design Applications.* Pitman Advanced Publishing Program. Boston, MA.

Prandtl, L., and Tietjens, O. G. (1957). *Fundamentals of Hydro- and Aeromechanics.* Dover Publications, New York, NY.

Tritton, D. J. (1982). *Physical Fluid Dynamics.* Van Nostrand Reinhold, Wokingham, Berkshire, England.

REPORT DOCUMENTATION PAGE

Form Approved
OMB No. 0704-0188

1. AGENCY USE ONLY *(Leave blank)*	2. REPORT DATE	3. REPORT TYPE AND DATES COVERED
	October 1997	Final report

4. TITLE AND SUBTITLE
Hydraulic Forces on a Wicket Gate Under Upstream Quasi-Laminar Flow

5. FUNDING NUMBERS

6. AUTHOR(S)
Luis A. de Béjar

7. PERFORMING ORGANIZATION NAME(S) AND ADDRESS(ES)
U.S. Army Engineer Waterways Experiment Station
3909 Halls Ferry Road
Vicksburg, MS 39180-6199

8. PERFORMING ORGANIZATION REPORT NUMBER
Technical Report SL-97-12

9. SPONSORING/MONITORING AGENCY NAME(S) AND ADDRESS(ES)
Headquarters, U.S. Army Corps of Engineers
Washington, DC 20310-000

10. SPONSORING/MONITORING AGENCY REPORT NUMBER

11. SUPPLEMENTARY NOTES
Available from National Technical Information Service, 5285 Port Royal Road, Springfield, VA 22161.

12a. DISTRIBUTION/AVAILABILITY STATEMENT
Approved for public release; distribution is unlimited.

12b. DISTRIBUTION CODE

13. ABSTRACT ***(Maximum 200 words)***

The two-dimensional potential theory of hydrodynamics is used to model the steady-state component of water flow approaching a gate aperture controlled by hydraulic wicket gates in a lock and dam system. The steady-state pressure against a typical wicket gate partially closing the aperture is then modeled using a conformal mapping technique in the complex plane. The elastic reaction at the supporting prop of the gate is derived from dynamic equilibrium considerations. The analytical results compare very well with the experiments conducted on a 1/25-scale physical model. A simple second-moment formulation allows the statistical characterization of response parameters for practical applications to design.

14. SUBJECT TERMS
First-Order-Second Movement
Hydrodynamics
Parameter characterization
Potential theory
Wicket gates

15. NUMBER OF PAGES
41

16. PRICE CODE

17. SECURITY CLASSIFICATION OF REPORT	18. SECURITY CLASSIFICATION OF THIS PAGE	19. SECURITY CLASSIFICATION OF ABSTRACT	20. LIMITATION OF ABSTRACT
UNCLASSIFIED	UNCLASSIFIED		

Destroy this report when no longer needed. Do not return it to the originator.